S2–S0 Spectroscopy of the van der Waals Complexes of Azulene with Rare Gases

ARTICLE *in* THE JOURNAL OF PHYSICAL CHEMISTRY A · MARCH 1996

Impact Factor: 2.69 · DOI: 10.1021/jp951823r

S_2-S_0 Spectroscopy of the van der Waals Complexes of Azulene with Rare Gases

Osama K. Abou-Zied, Hemant K. Sinha, and Ronald P. Steer*

Department of Chemistry, University of Saskatchewan, 110 Science Place, Saskatoon, Saskatchewan, Canada S7N 5C9

Received: July 3, 1995; In Final Form: November 17, 1995[⊗]

The S_2-S_0 fluorescence emission and excitation spectra of jet-cooled azulene and its complexes with the rare gases, Ne, Ar, Kr, and Xe, have been measured. Features due to $AZ{\cdot}RG_n$ ($n = 1-4$ when RG = Ar, Kr, Xe and $n = 1$ when RG = Ne) are observed in the S_2-S_0 fluorescence excitation spectra when azulene is coexpanded with the rare gases. The microscopic solvent shifts, $\delta\bar{\nu}$, of the origin bands for each complex scale linearly with the polarizability of the adatom(s), indicating that binding is dominated by dispersive interactions. This conclusion has been confirmed in calculations of the separate contributions of dispersion and induction to $\delta\bar{\nu}$. Mildly anharmonic progressions in very low frequency excited-state intermolecular (van der Waals) modes are attached to the origin bands of each $AZ{\cdot}Kr_n$ and $AZ{\cdot}Xe_n$ complex. The dominant progression is assigned to single quantum changes in that excited-state bending mode which involves motion of the adatom(s) in the plane perpendicular to the azulene ring containing the long (x) axis of the molecule. This assignment has been confirmed by calculating the frequencies of the bending and stretching vibrations in the ground state by using one-dimensional Morse and Taylor's series potential functions. The most stable geometries of the $n = 1-4$ complexes in their ground states have been calculated by using a summation of pairwise atom−atom Lennard-Jones 6−12 potentials. The potential minima of the 1:1 complexes are located over the seven-membered ring; no second minimum is found over the five-membered ring. The most stable 1:2 species appears to be the symmetric (1 + 1) complex in which one adatom is bound on each side of the azulene surface. Some evidence of the asymmetric (2 + 0) isomer is also found.

I. Introduction

Azulene, because of its exceptional behavior, occupies an important place in the development of our understanding of the spectroscopy and photophysics of closed-shell polyatomic organic molecules.[1−5] Unlike most aromatic hydrocarbons,[6] the S_1 state of azulene ($^1B_1$ in C_{2v} symmetry using the non-Mulliken convention) is almost nonfluorescent ($\phi_f(S_1) \sim 10^{-6}$)[7] and is very short-lived ($\tau(S_1) \sim 1$ ps),[8] whereas relatively strong fluorescence ($\phi_f(S_2) \sim 0.04$)[9] is observed from its second excited singlet state, S_2 ($^1A_1$), which is relatively long-lived ($\tau(S_2) \sim 1-2$ ns).[9]

Despite 50 years of study, important questions about the spectroscopy and excited-state dynamics of azulene and related compounds remain unanswered. In this paper we focus on matters concerning the S_2 state and its perturbation by solvent species in van der Waals complexes. The S_2-S_0 transition is electric dipole allowed, but the absorption, excitation, and emission spectra are complex, even when obtained for the bare molecule under cold, isolated conditions in a supersonic expansion.[10,11] These complexities have been attributed to intramolecular vibrational coupling associated with the vibronic mixing of S_2 with higher excited states (S_3 ($^1B_1$), S_4 ($^1A_1$), and S_5 ($^1B_1$)).[10−13] These couplings are further manifest in quantum interference effects in the spectrally-resolved fluorescence decays of the S_2 state.[14] Difficulties of interpretation notwithstanding, a review of the existing literature on azulene's S_2-S_0 and ground-state vibrational spectroscopy has revealed a surprising number of inconsistencies and errors in assignment for such a well-studied molecule. Our efforts to help remedy this situation will be the subject of a separate paper.[15]

The effects of structure and environment on azulene's excited-state dynamics have also been the subject of both recent and historical interest. Radiationless relaxation to S_1 dominates S_2's decay in condensed media and in the isolated molecule at low vibrational energies,[9,16] whereas parallel radiationless decay to S_0 is suggested to occur from higher vibrational states in the isolated parent, and perhaps to T_1 in some heavy-atom-substituted azulene derivatives.[16−18] Various medium-induced effects have also been reported.[9,17] Experiments in which van der Waals complexes of known structure and composition are synthesized and subjected to spectroscopic examination would appear to be a useful way of systematically studying the effects of modifying azulene's environment.

Comparisons between azulene, a weakly dipolar, nonalternant aromatic hydrocarbon, and its nonpolar, alternant structural isomer, naphthalene, are also of interest. The spectra and excited-state dynamics of van der Waals clusters of naphthalene with rare gases have been studied recently from both a theoretical[19,20] and an experimental[21,22] perspective. The source of the relatively small microscopic spectral shifts observed when naphthalene and other aromatic molecules with low S_1-S_0 oscillator strengths are complexed with the rare gases have been the object of particular interest.[23,24] In addition, the consequences of the presence of a very low barrier, at the center of mass of the bare chromophore, on the ground- and excited-state potential energy surfaces have been the focus of some attention.[19,20]

We have recently undertaken a series of experiments to measure the effects of complexation of small numbers of rare-gas atoms on the S_2-S_0 spectra and S_2 dynamics of azulene and a number of its simple derivatives. Here we present the results of our spectroscopic characterization of the van der Waals complexes of azulene with Ne, Ar, Kr, and Xe synthesized in a supersonic expansion. We also revisit the S_2-S_0 spectra of the bare chromophore and suggest several revisions to existing vibrational band assignments.

* To whom correspondence should be addressed.

[⊗] Abstract published in *Advance ACS Abstracts,* February 1, 1996.

0022-3654/96/20100-4375$12.00/0

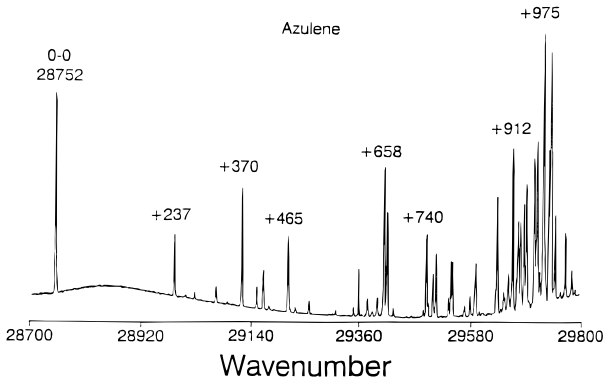

Figure 1. S_2-S_0 fluorescence excitation spectrum of jet-cooled azulene.

II. Experimental Section

The pulsed supersonic expansion, laser excitation, and fluorescence detection systems employed in these experiments have been described in detail elsewhere.[25,26] Briefly, the vapor from a heated solid sample of the chromophore is entrained in a stream of He to which a measured amount of rare gas has been added and is admitted to a high-vacuum chamber through a pulsed valve (Newport BV-100). Typical operating conditions are P(He) = 1−3 bar, P(rare gas) = $10^{-3}-10^{-1}$ bar, T(inlet) = 50−60 °C, repetition rate = 20 Hz, and nozzle diameter = 0.5 mm.

Excitation is effected by a XeCl excimer-pumped dye laser (Lumonics) operating on TMQ or PTP (Exciton) in dioxane which intercepts the expansion 5−10-mm downstream from the nozzle. When excitation spectra are measured, spatially filtered, undispersed emission is observed through a Schott WG 335 cutoff filter by using a cooled RCA C31034 photomultiplier coupled to a boxcar averager. Dispersed emission spectra are obtained by collecting the emission with a 4-in. diameter f:1 quartz lens and focusing it onto the entrance slit of a Heath-MacPherson EUE-700 series scanning monochromator equipped with a stepping motor. The signal from the photomultiplier detector (Hamamatsu R943-02) is further amplified by a preamplifier (SR 445) and is processed by a boxcar averager to improve signal to noise. Spectra with acceptable signal to noise at the required resolution are obtained by collecting emission from a sufficiently large number of excitation pulses per step, usually 50−100. Resolution of ca. 2 Å is obtained with the slit widths and step sizes most frequently employed in the present work.

Azulene (Aldrich) was used as received after determining that more highly purified material gave the same spectra. Ultrahigh purity helium (Matheson) and high purity Ne, Ar, Kr, and Xe (Matheson) were also used as received.

III. Results and Discussion

(a) Spectroscopy of Azulene. The S_2-S_0 fluorescence excitation spectrum of supersonically-expanded azulene was measured in the region $0_0^0 - 300$ cm^{-1} to $0_0^0 + 2000$ cm^{-1}. The segment of greatest interest in the present work, 0_0^0 to $0_0^0 + 1000$ cm^{-1}, is shown in Figure 1. Dispersed emission spectra were obtained by exciting several prominent bands in this spectrum; 28 752 cm^{-1} (0_0^0), + 237 cm^{-1} (39_0^1), + 370 cm^{-1} (17_0^1), + 465 cm^{-1} (38_0^1), + 658 cm^{-1} (16_0^1) and + 975 cm^{-1} (12_0^1) and overlapping bands). Both the excitation and emission spectra are in substantial agreement with the jet-cooled spectra reported by Fujii *et al.*[10] and by Lawrence and Knight.[11] In particular, we agree on the wavenumber of the origin, the wavenumbers of strong bands in the S_2-S_0 excitation and emission spectra, and most of the vibrational assignments. However, an examination of important additional details which can be observed in our S_2-S_0 spectra led us to discover some inconsistencies and errors in band assignments made in previous studies[10−14,16−18,27−37] of the spectroscopy and dynamics of azulene. None of these assignments involve bands which are crucial to the interpretation of the spectra of azulene's van der Waals complexes in the present work. Our contribution to resolving the discrepancies noted in the spectra of the bare molecule is the subject of a separate paper.[15]

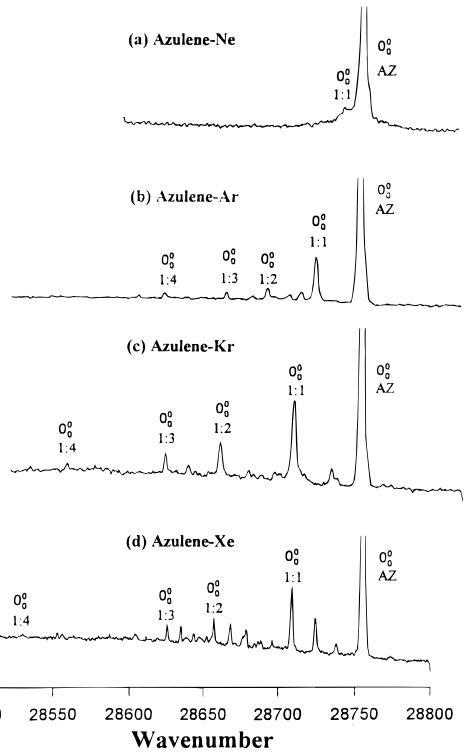

Figure 2. S_2-S_0 fluorescence excitation spectrum of azulene coexpanded with the rare gases: (a) Ne; (b) Ar; (c) Kr; (d) Xe. Origin bands of the AZ·RG$_n$ (n = 1−4) complexes are identified. Only the region to the red of the origin of the bare molecule is shown.

(b) Spectra of van der Waals Clusters and Microsolvation Shifts. In order to initiate a systematic study of the effects of molecular solvation on the spectra and the dynamics[38] of azulene, the van der Waals complexes AZ·RG$_n$ (RG = Ne, Ar, Kr, Xe) were synthesized by coexpanding the chromophore with suitable added partial pressures of the rare gases (RG). The resulting fluorescence excitation spectra in the region to the red of the S_2-S_0 origin of AZ, obtained by observing spectrally unresolved emission, are shown in Figure 2. By analogy with many other systems,[39−41] the weak bands lying immediately to the red of the origin of the bare molecule are assigned (*vide infra*) to the origin and progressions in one or more excited-state van der Waals vibrations of the n = 1−4 complexes. For AZ·Ne$_n$, only the n = 1 complex can be clearly identified. The strongest features to the red of each S_2-S_0 origin are, for each complex, replicated in regions to the red of other strong bands in the excitation spectra (not shown in Figure 2). For the Kr and Xe complexes, the bands immediately to the red of the origin of the bare chromophore may be grouped in several series. The first strong band, located $\delta\bar{\nu}$ to the red of the origin of the bare molecule, is assigned as the S_2-S_0 origin of the 1:1 complex. It is followed by one or more weaker bands, extending to higher wavenumbers, which are assigned to excited-state van der Waals vibrations. A moderately strong band located about $2\delta\bar{\nu}$ to the red of the origin of the bare molecule is assigned to

TABLE 1: Shifts of the S_2-S_0 Origin Bands in the 1:1, 1:2, 1:3, and 1:4 Azulene−Rare Gas Complexes[a]

RG	1:1	1:2[b]	1:3[c]	1:4[d]
Ne	−8.0			
Ar	−19.0	−40.0	−58.0	−86.5
Kr	−29.0	−61.5	−86.0	−129.5
Xe	−45.5	−97.5	−129.5	−224.5

[a] Values are in cm^{-1}. [b] For the 1 + 1 isomer. [c] For the 2 + 1 isomer. [d] For the 2 + 2 isomer. See text.

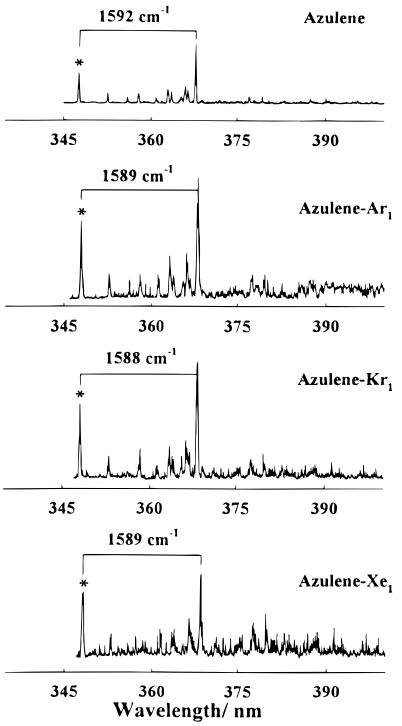

Figure 3. Dispersed S_2-S_0 fluorescence spectra of jet-cooled azulene and 1:1 AZ·RG complexes excited in their origin bands.

the S_2-S_0 origin of the symmetric 1:2 complex in which the two rare-gas atoms are located in equivalent positions on each side of the planar chromophore. This band also serves as the origin of at least one and, in the case of AZ·Xe_2, perhaps two progressions (*vide infra*) to higher wavenumbers. Very weak features assignable to the 1:3 and 1:4 complexes can also be seen when Ar, Kr, and Xe are coexpanded with AZ. The microscopic solvent shifts for the origin bands of identifiable $n = 1-4$ complexes are collected in Table 1.

Excitation at the origin bands of the 1:1 complexes of AZ with Ar, Kr, and Xe produced emission which was sufficiently intense to resolve spectroscopically. The emission spectra, obtained at ca. 2-Å resolution, are shown in Figure 3.

To aid in the assignments of the spectra of the van der Waals complexes, pressure of the rare gas in the expansion mixture was varied and the relative intensities of features assignable to various van der Waals complexes were plotted as a function of partial pressure. In all cases the relative intensities of all features assignable to cold bands of the same species showed similar behavior as a function of partial pressure.

We begin the analysis by considering the emission spectra, which are identical in each case to that of the bare molecule except for being offset to the red by $\delta\bar{\nu}$. Such spectra are typical of van der Waals complexes in which the adducts introduce low-frequency vibrations which are only weakly coupled to the much higher frequency vibrations of the chromophore. The emission spectra in Figure 3 therefore suggest that the van der Waals complexes of the rare gases with azulene in its S_2 state

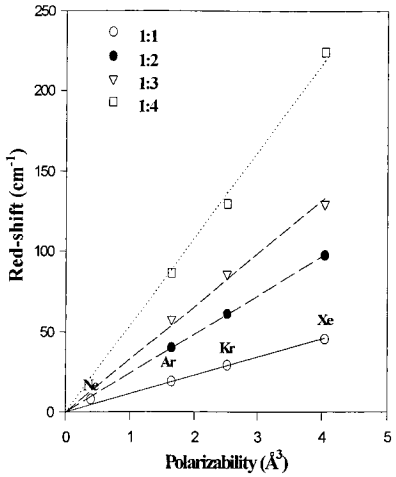

Figure 4. Observed red shift of the origin bands of the AZ·RG_n ($n = 1-4$) complexes vs the polarizability of the adatoms.

are not qualitatively different from those of the rare gases with the S_1 states of many other aromatic molecules.[39−41]

The measured microscopic solvation shifts, $\delta\bar{\nu}$, reveal a number of interesting features. First, the values of $\delta\bar{\nu}$ for the 1:1 to 1:4 complexes are directly proportional to the polarizabilities of the adatoms (Figure 4), as expected when dispersive forces dominate binding. The dispersive and inductive contributions to $\delta\bar{\nu}$, $\delta\bar{\nu}_{\text{disp}}$, and $\delta\bar{\nu}_{\text{ind}}$ can also be estimated by using the elementary theory of Longuet-Higgins and Pople.[42] According to their treatment

$$\delta\bar{\nu}_{\text{calc}} = \delta\bar{\nu}_{\text{disp}} + \delta\bar{\nu}_{\text{ind}} \tag{1}$$

where

$$\delta\bar{\nu}_{\text{disp}} = -\frac{\alpha_R}{3R_{MR}^6}\left\{\frac{I_M I_R}{I_M + I_R - E_M^{0-0}}\right\} \times \left\{\frac{E_M^{0-0}\alpha_M}{2(I_M + I_R)} + \frac{|R_{oi}|^2}{(4\pi\epsilon_o)^2 (I_R - E_M^{0-0})}\right\} \tag{2}$$

$$\delta\bar{\nu}_{\text{ind}} = -\frac{\alpha_R}{2R_{MR}^6}\left\{\frac{\mu_i^2 - \mu_o^2}{(4\pi\epsilon_o)^2}\right\} \tag{3}$$

Here α_R and α_M are the polarizabilities of the rare-gas atom and the chromophoric molecule, respectively, whose values are taken from refs 43 and 44. I_R and I_M are the ionization potentials of the rare-gas atoms and the chromophores with values from ref 43. R_{MR} is the distance between the centers of mass of M and R as determined by calculations based on a sum of Lennard-Jones 6−12 potentials (*vide infra*); the values used here are almost identical to those employed by Leutwyler *et al.*[45] for rare-gas complexes with carbazole, benzene, and other aromatic hydrocarbons. The quantities μ_i and μ_o are the permanent electric dipole moments of azulene in its upper (S_2) and ground (S_0) states; −0.358 D and +0.794 D, respectively.[44] R_{oi} is transition moment and is related to the radiative rate constant for the upper state via

$$|R_{oi}|^2 = g_i\left\{\frac{3\epsilon_o hc^3}{16\pi^3\nu^3}\right\}k_r \tag{4}$$

where k_r can be obtained from the upper-state lifetime, τ_i, and the emission quantum yield, ϕ_i, using $k_r = \phi_i/\tau_i$. The value of k_r, using accepted values of ϕ_i and τ_i,[16] is 1.31×10^7 s^{-1}.

TABLE 2: Calculated Microscopic Solvent Shifts of the S_2-S_0 Origin Bands of the 1:1 Complexes of Azulene with Rare Gases[a]

RG	$\delta\bar{\nu}_{disp}$	$\delta\bar{\nu}_{ind}$	$\delta\bar{\nu}_{calc}$	$\delta\bar{\nu}_{obs}$
Ne	−10.4	0.8	−9.7	−8.0
Ar	−23.3	1.6	−22.7	−19.0
Kr	−33.2	1.9	−31.3	−29.0
Xe	−41.9	2.3	−39.6	−45.5

[a] Values are in cm^{-1}.

The results of these calculations are given in Table 2. The agreement between the observed shifts, $\delta\bar{\nu}_{obs}$, and $\delta\bar{\nu}_{calc}$ is much better than expected, given the nature of the approximations made in developing this very elementary theory. Nevertheless the observed trends are correctly predicted and the dominance of dispersion in the binding of the RG atoms to AZ is confirmed.

The magnitude of $\delta\bar{\nu}$ for the 1:1 AZ·RG_n complexes also merits comment. Shalev *et al.*[40] have recently developed a semiempirical theory for predicting the electronic spectral shifts of aromatic molecule−rare-gas heteroclusters. Two classes of alternant aromatic molecules have been treated; those such as anthracene, tetracene, and perylene in which the S_0-S_1 transition is of the ^1L_a type and those such as naphthalene, phenanthrene, and pyrene in which the S_0-S_1 transition is of the ^1L_b type.[46] The latter excitations are weak because, within the framework of Hückel theory, they arise from the out-of-phase superposition of two zero-order one-electron excitations having the same intensity.[40] Extensive cancellation effects are found for excited-state interactions in such molecules and this is reflected in the observation of smaller spectral shifts in rare-gas clusters of alternant aromatic molecules exhibiting ^1L_b transitions than in those with ^1L_a transitions.[40]

Azulene presents an interesting comparison because it is a nonalternant aromatic hydrocarbon and does not have the pairing properties of Hückel orbitals in alternant molecules. As a result the S_0-S_1, ^1L_b, transition in azulene is polarized perpendicular to the C_2 axis and correlates with the S_0-S_2, ^1L_a, transition in its structural isomer, naphthalene.[22] Conversely, the S_0-S_2, $^1A_1$, transition in azulene is polarized parallel to the C_2 axis and has an excited state in which extensive interaction cancellation effects like those found in the S_1 state of naphthalene are expected. The observed spectral shifts in the AZ·RG_n complexes are about a factor of 2−3 smaller than those associated with alternant aromatic hydrocabons having ^1L_a transitions. The value of $\delta\bar{\nu}$ for the ^1L_b transition of the 1:1 complex of naphthalene with Ar is -14.0 cm^{-1},[22] compared with -19.0 cm^{-1} for the ^1L_a transition of AZ·Ar measured here. Clearly azulene in its S_2 state is behaving quantitatively like the S_1 states of naphthalene,[22] phenanthrene,[23] and pyrene,[24] despite the fact that the S_2-S_0 transition in azulene is of the ^1L_a type.

(c) Structures of the van der Waals Clusters. The structures and binding energies of the AZ·RG_n ($n = 1-4$) clusters in their ground electronic states were calculated by using Lennard-Jones "6−12" potential functions in a manner similar to that previously employed by several groups.[19,20,47,48] In these calculations, the atoms of the aromatic chromophore are assumed to be fixed at positions identical to those given by the X-ray structure (ref 49 for azulene), and the binding energy is calculated as a function of the position(s) of the adatom(s) on the molecule's surface(s). The binding energy at each geometry is calculated by a pairwise summation of attractive and repulsive atom−atom potentials, including adatom−adatom interactions when $n > 1$. Accordingly, the ground-state binding energy, *V(R)*, is given by

$$V(R) = \sum_u \sum_v (-A_{uv}R_{uv}^{-6} + B_{uv}R_{uv}^{-12}) \quad (5)$$

where A_{uv} and B_{uv} are empirically determined attractive and repulsive terms for the interactions between atoms u and v and the R_{uv} are the internuclear distances. The values of A_{uv} and B_{uv} are taken from Ondrechen *et al.*[47] Terms due to dipole-induced dipole interactions are not included but their contributions to the total binding energy are small. Variations in *V(R)* as a function of the position of the first adatom relative to the center of mass of the chromophore are shown in Figure 5 for the 1:1 AZ·Ar complex. The one-dimensional potentials for Ne, Kr, and Xe are qualitatively similar but differ in the depth of the potential wells. For the symmetric 1:2 complexes (1 + 1 configuration of the two adatoms), the first adatom was fixed at its equilibrium geometry and the second adatom was allowed to explore positions on the second, unsolvated side of the molecule. The binding energies and equilibrium geometries of the 1:1 and symmetric 1:2 complexes in their ground states are given in Table 3. Excited-state binding energies may be obtained by adding $|\delta\bar{\nu}|$ to the ground-state binding energy.

Additional features are found in the spectra of $n \geq 2$ complexes of Xe that are not observed in those of the other rare gases, and the AZ·Xe_n ($n \geq 2$) complexes were subject to further investigation for this reason. For the 1:2 unsymmetric species (2 + 0), an iterative procedure was used to find the location of the pair of Xe atoms at which binding was a maximum. For the (2 + 1) AZ·Xe_3 complex, the two adatoms on one side of the molecular surface were fixed at the equilibrium (2 + 0) locations found previously in the unsymmetric 1:2 complex, and the total binding energy was then calculated as a function of the position of the third Xe atom on the second surface.

The results of these calculations show that the interaction of the first adatom with the azulene surface produces a potential well with a single minimum located in the C_s plane at a point which resides above the seven-membered ring. Unlike naphthalene, no second minimum in the potential is present. The binding energies and the atom−molecule separation in the 1:1 species both increase with increasing size and polarizability of the adatom, as expected. The values of *z* (perpendicular distance from the adatom nucleus to the nuclear plane of the azulene) are comparable to those in other similar complexes.

In the symmetric 1:2 complexes the second adatom is located in a position which is structurally equivalent to that of the first adatom and the total binding energy is only slightly greater than twice the binding energy in the 1:1 complex (by 7, 9, and 15 cm^{-1} for Ar, Kr, and Xe, respectively). Transannular interaction in the (1 + 1) complexes is thus small, but significant. In the (2 + 0) isomer of AZ·Xe_2 the second atom displaces the first by 0.35 Å from its position in the 1:1 complex (to $x = 0.89$ Å). The second atom does not reside in the *xz* plane but is displaced toward carbon 1 (or 3) in the five-membered ring. The Xe−Xe distance is 4.35 Å in the most stable (2 + 0) isomer and the binding energy is 1600 cm^{-1}, 103 cm^{-1} less than that of the (1 + 1) isomer. The second atom is also 0.05 Å farther away from the azulene plane (at $z = 3.67$ Å) than the first. The most stable 1:3 complex is one of (2 + 1) configuration; the addition of a third atom to the (2 + 0) complex is bound with only slightly greater energy than the single adatom in the 1:1 complex. The most stable 1:4 complex is of (2 + 2) configuration.

(d) van der Waals Vibrations of the AZ·RG_n ($n = 1, 2$) Complexes. The complexation of a single adatom to a polyatomic molecule results in the conversion of the three translational degrees of freedom of the uncomplexed atom into

TABLE 3: Structures[a] and Binding Energies[b] of the Ground-State 1:1 and Symmetric 1:2 van der Waals Complexes of Azulene with Ne, Ar, Kr, and Xe

	RG_1				RG_2			
RG	*x*	*y*	*z*	energy	*x*	*y*	*z*	energy
Ne	0.70	0.00	2.94	−265	0.70	0.00	−2.94	−270
Ar	0.65	0.00	3.30	−567	0.65	0.00	−3.30	−574
Kr	0.65	0.00	3.44	−683	0.65	0.00	−3.44	−692
Xe	0.54	0.00	3.62	−844	0.54	0.00	−3.62	−859

[a] Coordinates are taken with respect to the center of mass of the azulene molecule in Å. See Figure 5 for a description of the coordinate system. [b] Binding energies are in cm^{-1}.

an additional three vibrational degrees of freedom in the 1:1 complex. These intermolecular or van der Waals modes are of low frequency and can be described in terms of the motion of the adatom parallel to Cartesian axes set in the framework of the polyatomic molecule. In 1:1 AZ·RG complexes these three intermolecular vibrations are the out-of-plane stretching vibration, parallel to the *z* axis, and two in-plane bending vibrations parallel to the long (*x*) and short (*y*) axes of the bare molecule. For rare gases such as Ar and Kr, bound to alternant aromatic hydrocarbons, the stretching vibrations often appear as short progressions of ca. 40−50 cm^{-1} spacing, whereas the bending vibrations are often in the 10−20-cm^{-1} range.[50] Short, mildly anharmonic progressions of between 14 and 17 cm^{-1} (fundamental) are observed for the 1:1 Kr and Xe complexes with azulene. The 1:1 complexes have C_s symmetry in which the *x* and *z* vibrations are of a′ character and the *y* bending vibration is of a″ character. The selection rules for vibrational quantum number changes accompanying the electric dipole allowed S_2-S_0 transition (in the 1:1 complex) are $\Delta v_{x,z} = 0, \pm1, \pm2, ...$ and $\Delta v_y = 0, \pm2, \pm4, ...$ Thus the observed progressions must be assigned to single quantum transitions in the "*x*" bending mode. This is in complete accord with the nature of the S_2-S_0 transition, which is polarized parallel to the *x* axis and which is expected to induce Franck−Condon activity because of the change in the magnitude and direction of the permanent dipole moment along the *x* axis (from +0.794 D to −0.358 D). No evidence of activity in the van der Waals stretching mode is found. Activity in the long axis bending, but not the stretching, mode is also found in the 1:1 complex of Ar with naphthalene.[22]

To confirm this assignment all three intermolecular vibrational frequencies of the ground state were calculated by using two different models to construct one-dimensional potential functions. First, the potentials in each of the three Cartesian coordinates were approximated by Morse functions of the form

$$V(R) = D_e(e^{-2\beta(R-R_o)} - 2e^{-\beta(R-R_o)}) \quad (6)$$

where D_e is the binding energy (measured from the bottom of the potential well), R_o is the perpendicular adatom−molecule distance when the adatom resides at the bottom of the well, and β is a parameter whose value is found empirically to give the best fit to the calculated Lennard-Jones potential. The vibrational constants are determined from

$$\omega_e = \beta\left\{\frac{D_e h}{2\pi^2 c\mu}\right\}^{1/2} \quad (7)$$

$$\omega_e x_e = \frac{\beta^2 h}{8\pi^2 c\mu} \quad (8)$$

In the second model a Taylor's series expansion about R_o was used to describe the lower, nearly harmonic portion of the potential. Thus

$$V(R) = V(R_o) + \frac{1}{2!}f_2\rho^2 + \frac{1}{3!}f_3\rho^3 + \frac{1}{4!}f_4\rho^4 + ... \quad (9)$$

where $\rho = R - R_o$ is the displacement and the f_n are the derivatives of the potential with respect to ρ evaluated at $\rho = 0$. Thus

$$\omega_e = \frac{1}{2\pi c}\left(\frac{k_{eff}}{\mu}\right)^{1/2} \quad (10)$$

$$\omega_e x_e = \frac{3h^2}{32\pi^4\omega_e{}^2\mu^2c^2}\left\{\frac{5f_3{}^2h}{8\pi^2\omega_e\mu c} - f_4\right\} \quad (11)$$

where k_{eff} is the effective harmonic force constant (equal to f_2), and μ is the reduced mass. The values of ω_e and $\omega_e x_e$ calculated by each method for fixed azulene are given in Table 4. Clearly single quantum transitions to v'_x vibrational levels in a slightly displaced, slightly deeper upper state potential well are completely consistent with the observed progressions.

Significant anharmonicity is observed in the 1:1 AZ·Xe progression, as might be expected given the shape of the potential function, which has a minimum over the seven-membered ring and a more gently sloping portion toward the five-membered ring in the *x* direction.

The intermolecular vibrational structure in the 1:2 complexes $AZ·Kr_2$ and $AZ·Xe_2$ is particularly interesting; that for $AZ·Xe_2$ is shown in Figure 6. For these complexes, strong features ca. $2\delta\bar{\nu}$ to the red of the origin of the bare molecule are clearly due to the origin of the symmetric (1 + 1) complex. This species has C_{2v} symmetry. The two adatoms provide six additional vibrational degrees of freedom, two stretching and four bending modes. The separation of ca. 10 cm^{-1} between adjacent bands in the progression built on this origin precludes its assignment to either the symmetric or asymmetric stretches. The four bending vibrations consist of one a_1 vibration, in which the two adatoms move symmetrically in the plane perpendicular to the azulene plane, i.e., parallel to azulene's long (*x*) axis, and three non-totally-symmetric bends, one each of a_2, b_1, and b_2 character. The selection rule for the a_1 vibration is $\Delta v = 0, \pm1, \pm2, ...$ whereas $\Delta v = 0, \pm2, \pm4, ...$ applies to the non-totally-symmetric bends. Thus the progression built on the origin of the symmetric 1:2 species must involve single quantum transitions in the totally symmetric bend. The Franck−Condon profile of this progression, which can be seen most clearly in the $AZ·Xe_2$ spectrum, is consistent with a transition to a slightly *x*-displaced, mildly anharmonic oscillator in the S_2 state.

A second set of bands is also present in the 1:2 complex, beginning with a weak band slightly to the red of the $v'(a_1) = 2$ band in the progression associated with the (1 + 1) species described above. This weak band could be either the $\Delta v = 2$ transition for one of the non-totally-symmetric bends in the (1 + 1) species (likely the b_1 bend) or the origin band of the unsymmetric (2 + 0) isomer. The latter interpretation is suggested by the fact that the (2 + 0) isomer is less stable than the (1 + 1) isomer, consistent with the smaller red shift and lower intensity of these bands. Moreover, the incremental red shift from the origin of the 1:1 species to this band (32.0 cm^{-1} in the $AZ·Xe_n$ system) is the same as the incremental red shift from the origin of the symmetric (1 + 1) 1:2 species to the origin of the (2 + 1) 1:3 complex. However, this interpretation would require that the remaining weak bands immediately to the blue form a progression similar to that seen in the (2 + 1)

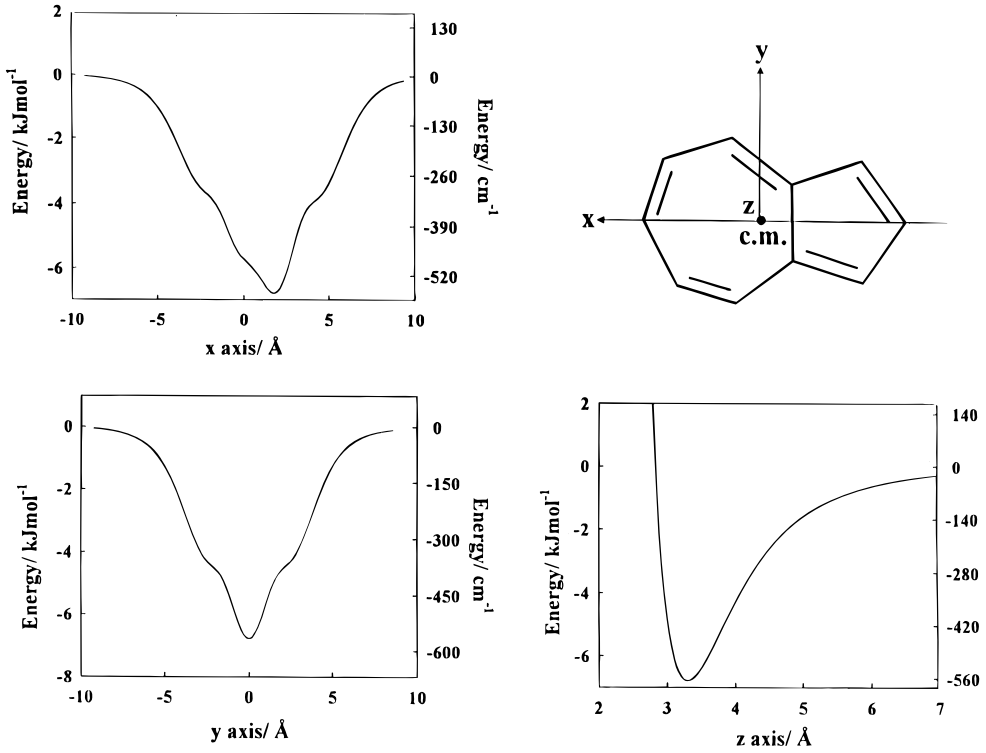

Figure 5. One-dimensional potentials for the AZ·Ar_1 complex calculated by using the sum of Lennard-Jones 6−12 atom−atom potentials. The coordinate system, shown upper right, has its origin at the center of mass of the bare azulene molecule.

TABLE 4: Wavenumbers of van der Waals Fundamental Vibrations Observed in 1:1 AZ-RG Complexes and Calculated by Using Morse and Taylor's Series Potentials

		Morse[a]			Taylor's series[a]		
RG	$\bar{\nu}_{obs}$[a]	*x*	*y*	*z*	*x*	*y*	*z*
Ar	not obs	18.5(0.15)	14.9(0.10)	49.8(1.1)	15.8(0.11)	16.4(0.19)	51.6(1.7)
Kr	16.5	14.9(0.08)	12.0(0.05)	44.3(0.69)	12.7(0.05)	12.9(0.11)	42.6(1.2)
Xe	15.5(1.0)	13.2(0.05)	10.9(0.03)	43.1(0.52)	10.0(0.08)	11.6(0.09)	39.9(1.3)

[a] The wavenumber of the fundamental vibration is followed in parentheses by the anharmonicity.

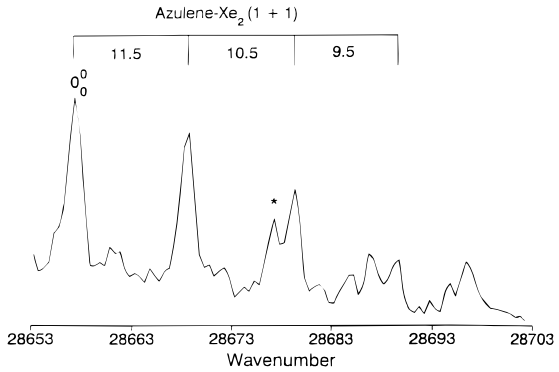

Figure 6. Detail of the vibrational structure in the S_2-S_0 fluorescence excitation spectrum of AZ·Xe_2. The starred band is discussed in the text.

complex, and this does not appear to be the case. Further work is therefore required to assign these bands with certainty.

IV. Conclusions

The S_2-S_0 fluorescence emission and excitation spectra of jet-cooled azulene and its complexes with the rare gases, Ne, Ar, Kr, and Xe, have been measured. Features due to AZ·RG_n ($n = 1-4$ when RG = Ar, Kr, Xe and $n = 1$ when RG = Ne) are observed in the S_2-S_0 fluorescence excitation spectra when azulene is coexpanded with the rare gases. The microscopic solvent shifts, $\delta\bar{\nu}$, of the origin bands for each complex scale linearly with the polarizability of the adatom(s), indicating that binding is dominated by dispersive interactions. This conclusion is confirmed in calculations, based on the formalism of Longuet-Higgins and Pople, of the separate contributions of dispersion and induction to $\delta\bar{\nu}$.

Mildly anharmonic progressions in very low frequency excited-state intermolecular (van der Waals) modes are attached to the origin bands of each AZ·Kr_n and AZ·Xe_n complex. The dominant progression is assigned to single quantum changes in that excited-state bending mode which involves motion of the adatom(s) in the plane perpendicular to the azulene ring containing the long (*x*) axis of the molecule. This assignment is confirmed by calculations of the frequencies of the bending and stretching vibrations in the ground state using one-dimensional Morse and Taylor's series potential functions.

The most stable geometries of the $n = 1-4$ complexes in their ground states were calculated by using a summation of pairwise atom−atom Lennard-Jones 6−12 potentials. The potential minima of the 1:1 complexes are located over the seven-membered ring; no second minimum is found over the five-membered ring. The most stable 1:2 species appears to be the symmetric (1 + 1) complex in which one adatom is bound on each side of the azulene surface. Some evidence of the asymmetric (2 + 0) isomer is also found.

Acknowledgment. We are grateful to the Natural Sciences and Engineering Research Council of Canada and the Centers of Excellence for Molecular and Interfacial Dynamics for

financial support. We are also grateful to Dr. Robert Weersink, University of Toronto, for providing a computer program for calculating the Lennard-Jones potentials.

References and Notes

(1) Beer, M.; Longuet-Higgins, H. C. *J. Chem. Phys.* **1955**, *23*, 1390.
(2) Sidman, J.W.; McClure, D.S. *J. Chem. Phys.* **1956**, *24*, 757.
(3) Viswanath, G.; Kasha, M. *J. Chem. Phys.* **1956**, *24*, 574.
(4) Hunt, G.R.; Ross, I.G. *Proc. Chem. Soc.* **1961**, *11*.
(5) Shank, C.V.; Ippen, E.P.; Teschke, O.; Fork, R.L. *Chem. Phys. Lett.* **1978**, *57*, 433.
(6) Kasha, M. *Discuss. Faraday Soc.* **1950**, *9*, 14.
(7) Rentzepis, P.M. *Chem. Phys. Lett.* **1969**, *3*, 717.
(8) Wagner, B.D.; Szymanski, M.; Steer, R.P. *J. Chem. Phys.* **1993**, *98*, 301.
(9) Wagner, B.D.; Tittelbach-Helmrich, D.; Steer, R.P. *J. Phys. Chem.* **1992**, *96*, 7904.
(10) Fujii, M.; Ebata, T.; Mikami, N.; Ito, M. *Chem. Phys.* **1983**, *77*, 191.
(11) Lawrence, W.D.; Knight, A.E.W. *J. Phys. Chem.* **1990**, *94*, 1249.
(12) Orlandi, G.; Zerbetto, F. *Chem. Phys.*, **1987**, *113*, 167.
(13) Negri, F.; Zgierski, M.Z. *J. Chem. Phys.* **1993**, *99*, 4318.
(14) Demmer, D.R.; Hager, J.W.; Leach, G.W.; Wallace, S. C. *Chem. Phys. Lett.* **1987**, *136*, 329.
(15) Abou-Zied, O.K.; Sinha, H.K.; Steer, R.P., *J. Mol. Spectrosc.*, submitted for publication.
(16) Woudenberg, T.M.; Kulkarni, S.K.; Kenny, J.E. *J. Chem. Phys.* **1988**, *89*, 2789.
(17) Eber, G.; Schneider, S.; Dörr, F. *Chem. Phys. Lett.* **1977**, *52*, 59.
(18) Hirata,Y.; Lim, E.C. *J. Chem. Phys.* **1978**, *69*, 3292.
(19) Troxler, T.; Leutwyler, S. *J. Chem. Phys.* **1993**, *99*, 4363.
(20) Mandziuk, M.; Bacic, Z. *J. Chem. Phys.* **1993**, *98*, 7165.
(21) Troxler, T.; Leutwyler, S. *Ber. Bunsenges. Phys. Chem.* **1992**, *96*, 1246.
(22) Troxler, T.; Leutwyler, S. *J. Chem. Phys.* **1991**, *95*, 4010.
(23) Troxler, T.; Knockenmuss, R.; Leutwyler, S. *Chem. Phys. Lett.* **1989**, *159*, 554.
(24) Furlan, A.; Troxler, T.; Leutwyler, S. *J. Phys. Chem.* **1993**, *97*, 13527.
(25) Ludwiczak, M.; Latimer, D.R.; Steer, R.P. *J. Mol. Spectrosc.* **1991**, *147*, 414.
(26) Sinha, H.K.; Steer, R.P. *Chem. Phys. Lett.* **1993**, *211*, 397.
(27) Chao, R.S.; Khanna, R.K. *Spectrochim. Acta* **1977**, *33A*, 53.
(28) Hochstrasser, R.M.; Nyi, C.A. *J. Chem. Phys.* **1979**, *70*, 1112.
(29) van Tets, A.; Gunthard, Hs. H. *Spectrochim. Acta* **1963**, *19*, 1495.
(30) van Tets, A.; Gunthard, Hs. H. *Spectrochim. Acta* **1972**, *28A*, 1759.
(31) Steele, D. *J. Mol. Spectrosc.* **1965**, *15*, 333.
(32) Steele, D. *Spectrochim. Acta* **1966**, *22*, 1275.
(33) Hunt , G.R.; Ross, I.G. *J. Mol. Spectrosc.* **1959**, *3*, 604.
(34) Small, G.J.; Kusserow, S. *J. Chem. Phys.* **1974**, *60*, 1558.
(35) Bevilacqua, A.C.; Cho, C.H.; Kenny, J.E. *Spectrochim. Acta* **1988**, *44A*, 293. Bevilacqua, A.C. Ph.D. Thesis, Tufts University, 1991. Kenny, J.E., private communication.
(36) Cable, J.R.; Albrecht, A.C. *J. Chem. Phys.* **1986**, *84*, 1969.
(37) Bree, A.; Pal, A.J.; Taliani, C. *Spectrochim. Acta* **1990**, *46A*, 1767.
(38) Abou-Zied, O.; Demmer, D.R.; Wallace, S.; Steer, R.P., in preparation.
(39) Boesiger, J.; Leutwyler, S. *Chem. Phys. Lett.* **1986**, *126*, 238.
(40) Shalev, E.; Ben-Horin, N.; Even, U.; Jortner, J. *J. Chem. Phys.* **1991**, *95*, 3147; Shalev, E.; Ben-Horin, N.; Jortner, J. *J. Chem. Phys.* **1992**, *96*, 1848.
(41) Ludwiczak, M.; Sinha, H.K.; Steer, R.P. *Chem. Phys. Lett.* **1992**, *194*, 196.
(42) Longuet-Higgins, H.; Pople, J. *J. Chem. Phys.*, **1957**, *27*, 192.
(43) Lide, D.R.; Frederikse, H.P.R. *CRC Handbook of Chemistry and Physics*, 74th ed.; London, 1993−1994.
(44) Baumann, W. *Chem. Phys.* **1977**, *20*, 17.
(45) Leutwyler, S. *Chem. Phys. Lett.* **1984**, *107*, 284.
(46) Jaffé, H.H.; Orchin, M. *Theory and Applications of Ultraviolet Spectroscopy*, Wiley: New York, 1962.
(47) Ondrechen, M.; Berkovitch-Yellin, Z.; Jortner, J. *J. Am. Chem. Soc.* **1981**, *103*, 6568.
(48) Menapace, J.A.; Bernstein, E.R. *J. Phys. Chem.* **1987**, *91*, 2533.
(49) Robertson, J.M.; Shearer, H.M.M.; Sim, G.A.; Watson, D.G. *Acta Crystallogr.* **1962**, *15*, 1; **1965**, *18*, 565.
(50) Even, U.; Amirav, A.; Leutwyler, S.; Ondrechen, M.; Berkovitch-Yellin, Z.; Jortner, J. *Faraday Discuss. Chem. Soc.* **1982**, *73*, 153.

JP951823R